World Electric Vehicle Journal

MDPI

Article

Comparison of the Economic and Environmental Performance of V2H and Residential Stationary Battery: Development of a Multi-Objective Optimization Method for Homes of EV Owners

Ryosuke Kataoka [1,*], Akira Shichi [1], Hiroyuki Yamada [1], Yumiko Iwafune [2] and Kazuhiko Ogimoto [2]

[1] Toyota Central R&D Labs., Inc., 41-1, Yokomichi, Nagakute, Aichi 480-1192, Japan; a-shichi@mosk.tytlabs.co.jp (A.S.); e1581@mosk.tytlabs.co.jp (H.Y.)

[2] The University of Tokyo, 4-6-1, Komaba, Meguro-ku, Tokyo 153-8505, Japan; iwafune@iis.u-tokyo.ac.jp (Y.I.); ogimoto@iis.u-tokyo.ac.jp (K.O.)

* Correspondence: r-kataoka@mosk.tytlabs.co.jp; Tel.: +81-564-71-7447

Received: 10 October 2019; Accepted: 14 November 2019; Published: 15 November 2019

Abstract: The use of batteries of electric vehicles (EVs) for home electricity applications using a bidirectional charger, a process called vehicle-to-home (V2H), is attracting the attention of EV owners as a valuable additional benefit of EVs. To motivate owners to invest in V2H, a quantitative evaluation to compare the performance of EV batteries with that of residential stationary batteries (SBs) is required. In this study, we developed a multi-objective optimization method for the household of EV owners using energy costs including investment and CO_2 emissions as indices and compared the performances of V2H and SB. As a case study, a typical detached house in Japan was assumed, and we evaluated the economic and environmental aspects of solar power self-consumption using V2H or SB. The results showed that non-commuting EV owners should invest in V2H if the investment cost of a bidirectional charger is one third of the current cost as compared with inexpensive SB, in 2030. In contrast, our results showed that there were no advantages for commuting EV owners. The results of this study contribute to the rational setting of investment costs to increase the use of V2H by EV owners.

Keywords: electric vehicle; vehicle-to-home; multi-objective optimization; optimal sizing; optimal scheduling; solar power self-consumption

1. Introduction

The widespread use of electric vehicles (EVs) is essential to respond to the 2 °C scenario. Japan has set the ambitious goal of raising the total percentage of EV and plug-in hybrid vehicle (PHV) stock to 16% by 2030 [1]. Improving the value of EVs and PHVs by using them to contribute to the supply-and-demand balance of electric power systems, including variable renewable energy sources, is one solution proposed as a means of accelerating their spread. Representative technological examples of this approach are vehicle-to-grid (V2G) and vehicle-to-home (V2H) systems. V2G can be applied to use the batteries of EVs to operate power grids. In contrast, V2Hs use the batteries of EVs for energy management in the domain of behind-the-meter systems such as the home of an EV owner. Therefore, V2H can provide benefits to EV owners with a simple and small-scale system as compared with V2G. To clarify the benefits of V2H, a quantitative evaluation of the economics of V2H systems has been performed in some recent studies.

Previous studies have focused on combinations of residential photovoltaic (PV), stationary battery (SB), and V2H technology and have performed economical evaluations by optimizing the associated operational schedules. The impact of SB and EV charging and discharging schedules on the economics in houses with PV, V2H, and SB has been evaluated [2]. The revenue generated from power trading under the DR program using PV, SB, and EV has also been analyzed [3]. Furthermore, the economics of EV charging and discharging schedule have been analyzed using a model that considers the uncertainty of PV power generation and EV trips [4]. Some studies have focused on the optimal sizing of equipment to evaluate the economics considering capital investment costs. The optimal size of PV and SB in homes with V2H under dynamic pricing have been examined [5]. In addition, the economically optimal size of battery capacity and maximum power has been derived considering each investment cost [6]. Monte Carlo simulation has also been used to evaluate the economically optimal sizing of PV, wind, and SB in a house with V2H [7].

The previous studies described above only assessed the economic value based on the premise of introducing V2H. V2H can be realized using a bidirectional charger, e.g., CHAdeMO protocol. In other words, whether an EV owner will invest in a bidirectional charger was not considered in these studies. HEV-TCP by IEA lists the investment cost of a bidirectional charger as a barrier to the spread of V2H [8]. Clarifying the value of V2H could help motivate EV owners to introduce bidirectional chargers. In addition, if a SB is enough inexpensive, V2H may not be selected by the EV owners. Therefore, to motivate EV owners to invest in V2H, it is necessary to economically evaluate V2H including the investment cost of bidirectional chargers as compared to SBs.

Additionally, consumer tastes are diversifying. A multi-optimization method, targeting both environmental and economic issues, is necessary to develop an optimum plan for environmentally oriented owners. A multi-objective scheduling method has been proposed to minimize the total operational costs and emissions in a distribution network [9]. However, the multi-objective optimization methods used previously did not focus on energy management of the EV owner's home in conjunction with V2H.

In this study, we examine whether V2H is economically and environmentally rational for EV owners as compared to residential SBs, including the investment cost of the bidirectional charger. Specifically, a multi-objective optimization method is developed to derive the optimal operation schedule and the size of equipment, such as PV and SB, to be installed in the home, using the home energy costs and CO_2 emissions as indices. The method is formulated in a mixed integer linear programming (MILP) framework, which generalizes the model constructed by the authors [10]. The case study analyzes the sensitivity of the cost of the bidirectional charger to a low-cost SB in the future, assuming different uses of EV. The results of this study provide guidance on the future cost targets of bidirectional chargers to motivate EV owners.

2. Method

2.1. Modeling

The energy flow structure of the household is presented in Figure 1. This structure includes a residential PV, SB, EV, and EV discharging (V2H) as the power supply and demand from the grid to the residential power demand. The sources of power supply are the grid and PV. The power demand to drive the EV is divided from the residential power demand. The SB can be used for residential power demand or EV charging. The EV battery can be used not only for driving but also for residential power demand with the V2H option. Selling back to the grid is only possible from the PV.

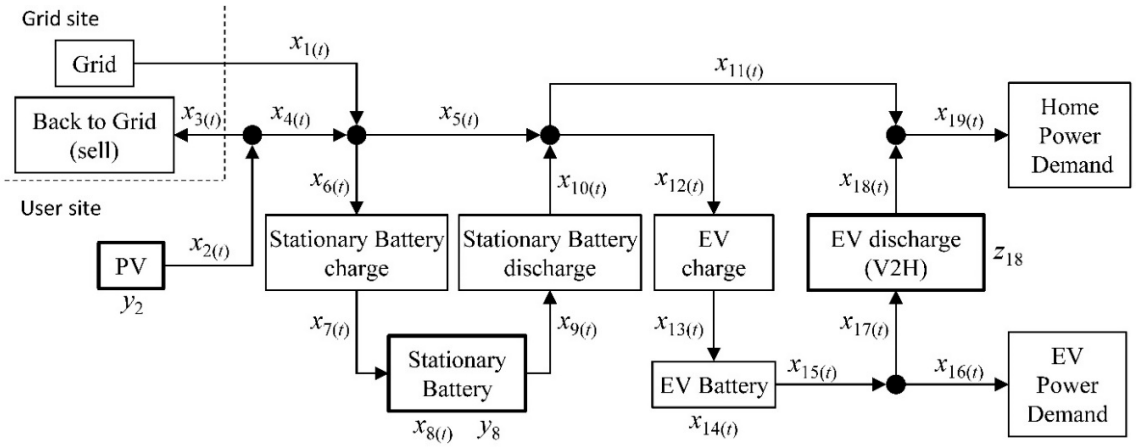

Figure 1. Energy flow structure of the household.

This structure is formulated as a multi-objective optimization problem based on MILP. We use this formula to optimize energy flow at hourly granularity and capital investment based on perfect forecasts of the residential power demand, the power demand of EV, and PV power generation. The optimization indicators are total energy costs and CO_2 emissions at home. Equation (1) shows the objective function to minimize the weighted sum of the cost and CO_2 emissions:

$$F(x_1, x_3, y_2, y_8, z_{18}) = w\frac{f_{cost}(x_1, x_3, y_2, y_8, z_{18})}{\min\{f_{cost}(x_1, x_3, y_2, y_8, z_{18})\}} + (1-w)\frac{f_{co2}(x_1)}{\min\{f_{co2}(x_1)\}} \quad (1)$$

where x_1 and x_3 represent the hourly amount of energy purchased from the grid and sold back to the grid, respectively; y_2 and y_8 denote the size of PV and SB, respectively; and z_{18} represents the binary variable, which denotes the investment for the bidirectional charger for V2H (z_{18} = 0 when not investing in a bidirectional charger, and z_{18} = 1 when investing in a bidirectional charger). A set of Pareto solutions related to the economy and environment can be calculated with the weight value w from 0 to 1, i.e., the minimum CO_2 solution is when w = 0, and the minimum cost solution is when w = 1. In Equation (1), f_{cost} represents the total energy cost during the time horizon of the optimization problem T (hour) and is calculated using the sum of the grid purchase costs, the income from selling power to the grid, and the equipment costs as follows:

$$f_{cost} = \sum_{t=1}^{T}\left\{p_{buy}(t)\cdot x_1(t) - p_{sell}(t)\cdot x_3(t)\right\} + (C_{PV}\cdot y_2 + C_{SB}\cdot y_8 + C_{V2H}\cdot z_{18})\cdot T \quad (2)$$

where price fluctuations such as dynamic prices can be considered by giving an exogenous value at time t (hourly granularity) to the purchase unit price $p_{buy}(t)$ and the selling unit price $p_{sell}(t)$. C_{PV}, C_{SB}, and C_{V2H} are cost coefficients of PV, SB, and the bidirectional charger of base size (1 kW, 1 kWh, and 1 unit, respectively), and these values include the investment and maintenance costs as follows:

$$C_{PV} = \left(\frac{I_{PV}}{L_{PV}} + M_{PV}\right)/8760 \quad (3)$$

$$C_{SB} = \left(\frac{I_{SB}}{L_{SB}} + M_{SB}\right)/8760 \quad (4)$$

$$C_{V2H} = \left(\frac{I_{V2H}}{L_{V2H}} + M_{V2H}\right)/8760 \quad (5)$$

where, I_{PV}, I_{SB}, and I_{V2H} are investment costs; L_{PV}, L_{SB}, and L_{V2H} are the product life (in years); and M_{PV}, M_{SB}, and M_{V2H} are annual maintenance costs. The value 8760 in Equations (3) to (5) refers to

the number of hours in a year. Notably, the investment and other costs of the EV are not included because it is assumed to be an independent investment for mobility reasons only. In Equation (1), f_{co2} represents the total CO_2 emission from the grid power during the time horizon of the optimization problem T and is calculated by Equation (6).

$$f_{CO_2} = \sum_{t=1}^{T} e_{grid} \cdot x_1(t) \tag{6}$$

The optimization constraints are expressed as: Equations (7) to (28), including the balance of supply and demand, the power of equipment, storage, junctions, charging or discharging efficiency, and availability of EV. Equation (7) states that the power supply from PV $x_2(t)$ can be calculated by the normalized power production $P_{PV\_unit}(t)$ and the size of PV y_2.

$$x_2(t) = P_{PV\_unit}(t) \cdot y_2 \tag{7}$$

Equations (8) and (9) state that $x_{16}(t)$ and $x_{19}(t)$ are always equivalent to the power demands $D_{EV}(t)$ and $D_{home}(t)$, respectively. $P_{PV\_unit}(t)$, $D_{EV}(t)$, and $D_{home}(t)$ are provided as exogenous variables. In other words, they are perfectly predicted in the optimization process.

$$x_{16}(t) = D_{EV}(t) \tag{8}$$

$$x_{19}(t) = D_{home}(t) \tag{9}$$

Equations (10) to (14) represent the equation of continuity at the junctions.

$$x_2(t) = x_3(t) + x_4(t) \tag{10}$$

$$x_1(t) + x_4(t) = x_5(t) + x_6(t) \tag{11}$$

$$x_5(t) + x_{10}(t) = x_{11}(t) + x_{12}(t) \tag{12}$$

$$x_{11}(t) + x_{18}(t) = x_{19}(t) \tag{13}$$

$$x_{15}(t) = x_{16}(t) + x_{17}(t) \tag{14}$$

Equations (15) to (18) represent the efficiency of charging or discharging ($\eta_{SB\_Ch.}\ \eta_{SB\_DisCh.} < 1$, $\eta_{EV\_Ch.}\ \eta_{EV\_DisCh.} < 1$).

$$x_7(t) = \eta_{SB\_Ch.} \cdot x_6(t) \tag{15}$$

$$x_{10}(t) = \eta_{SB\_DisCh.} \cdot x_9(t) \tag{16}$$

$$x_{13}(t) = \eta_{EV\_Ch.} \cdot x_{12}(t) \tag{17}$$

$$x_{18}(t) = \eta_{EV\_DisCh.} \cdot x_{17}(t) \tag{18}$$

Equations (19) and (20) state that the state of charge (SoC) of the batteries (SB and EV) are dependent on the charging or discharging history, as follows:

$$x_8(t) = x_8(t-1) + x_7(t) - x_9(t) \tag{19}$$

$$x_{14}(t) = x_{14}(t-1) + x_{13}(t) - x_{15}(t) \tag{20}$$

where the initial values $x_8(0)$ and $x_{14}(0)$ are given as a predetermined ratio $r_{SB\_ini.}$ and $r_{EV\_ini.}$ to the capacity sizes (i.e., $x_8(0) = y_8\ r_{SB\_ini.}$ and $x_{14}(0) = Cap._{EV}\ r_{EV\_ini.}$). In addition, the SoC of the batteries has a lower and upper limit, as follows:

$$0 \le x_8(t) \le y_8 \tag{21}$$

$$lb_{EV\_SOC} \leq x_{14}(t) \leq ub_{EV\_SOC} \tag{22}$$

where lb_{EV_SOC} and ub_{EV_SOC} are given from the specification of the EV.

Equations (23) to (26) denote the limit of charging or discharging power of SB or EV. The charging and discharging power of SB are limited by the rates of capacity size given by Equations (23) and (24).

$$0 \leq x_7(t) \leq r_{SB\_Ch.} \cdot y_8 \tag{23}$$

$$0 \leq x_9(t) \leq r_{SB\_DisCh.} \cdot y_8 \tag{24}$$

In contrast, the EV can be charged or discharged when the EV is parked at home, i.e., the charging and discharging powers are given as follows:

$$0 \leq x_{12}(t) \leq P_{EV\_Ch.} \cdot \delta_{EV}(t) \tag{25}$$

$$0 \leq x_{13}(t) \leq P_{EV\_DisCh.} \cdot \delta_{EV}(t) \tag{26}$$

where $P_{EV\_Ch.}$ and $P_{EV\_DisCh.}$ are the maximum power of the EV charger and discharger, and $\delta_{EV}(t)$ is a binary parameter that represents the absence of the EV based on its driving pattern ($\delta_{EV}(t) = 0$ while the EV is absent, and $\delta_{EV}(t) = 1$ while the EV is parked at home).

Equations (27) and (28) represent the maximum sizes of PV and SB.

$$0 \leq y_2 \leq PV_{max} \tag{27}$$

$$0 \leq y_8 \leq SB_{max} \tag{28}$$

To obtain a set of Pareto solutions, the optimization equations are adopted in the following three steps:

1. To obtain $min\{f_{cost}(x_1, x_3, y_2, y_8, z_{18})\}$ in Equation (1), the problem takes the following form:

$$\begin{gathered}\text{min. objective function Equation (2)} \\ \text{subject to: optimization constraints Equations (7) to (28)}\end{gathered} \tag{29}$$

2. To obtain $min\{f_{co2}(x_1)\}$ in Equation (1), the problem takes the following form:

$$\begin{gathered}\text{min. objective function Equation (3)} \\ \text{subject to: optimization constraints Equations (7) to (28)}\end{gathered} \tag{30}$$

3. Substitute $min\{f_{cost}(x_1, x_3, y_2, y_8, z_{18})\}$ and $min\{f_{co2}(x_1)\}$ calculated in the previous two steps into Equation (1) to solve the problem described as following form:

$$\begin{gathered}\text{min. objective function Equation (1)} \\ \text{subject to: optimization constraints Equations (7) to (28)}\end{gathered} \tag{31}$$

The MILP problem described in Equations (29) to (31) is a classical optimization paradigm and can be solved using algorithms, such as the branch and bound method.

2.2. Sample System

To compare the future V2H and SB economically and environmentally, Japanese EV owners living in a detached house are chosen as typical case studies, in 2030. The time horizon of the optimization problem, T, and the start time are set to one year (8760 h) and 0:00 in April 1, respectively. The eight cases comprising two EV driving patterns and four combinations of equipment are evaluated, as shown in Table 1. To compare the impact of different driving patterns on the economic and environmental rationality of V2H, non-commuter and commuter cars were considered. In case 1, the power supply from the grid meets the residential electricity demand and the non-commuter EV demand without an investment in equipment. Case 2 adds the option of an investment in PV to case 1. Cases 3 and 4 add investment options of SB and bidirectional chargers for V2H to case 2, respectively. In cases 5 to 8, the driving pattern assumed is that of a commuter car. In cases 4 and 8, to explicitly compare the effect of investment in V2H with the results of other cases, the necessity of a bidirectional charger z_{18} is forcibly given as 1 and an optimization calculation is performed. All the case studies are conducted using the MATLAB Optimization Toolbox [11] as a solver based on the branch and bound method.

Table 1. Combinations to be optimized.

Case	EV Driving Pattern	System Configurations			
		Grid	PV	SB	V2H
1	Non-commuter	○	-	-	-
2		○	○	-	-
3		○	○	○	-
4		○	○	-	○
5	Commuter	○	-	-	-
6		○	○	-	-
7		○	○	○	-
8		○	○	-	○

In this study, the EV driving patterns are given as exogenous variables in the optimization process. Therefore, this study evaluates an upper bound on the benefits that can be earned through the V2H options. In reality, the value will be reduced due to EV availability forecasting error and range anxiety. The one-year driving pattern of the non-commuter EV is estimated using Equations (32) to (35), assuming that trips occur randomly with reference to the data based on a country-wide survey [12]. That is, the departure time (DT) is given by the probability shown in Figure 2, and the comeback time (CT) is obtained by adding the stay time (ST) and driving period (DP) to DT, as follows:

$$CT = DT + \frac{ST + 2 * DP}{60} \tag{32}$$

$$ST = N(60,\ 15) \tag{33}$$

$$DP = \frac{TL}{V * 60} \tag{34}$$

$$TL = \left|N(8,\ 3)\right| \tag{35}$$

where ST and trip length (TL) are calculated by random variables with a normal distribution. The average driving speed, V, is set to 30 km/h. Therefore, Figure 3a shows the existence ratio of the non-commuter EV at home. The annual mileage of the non-commuter EV is estimated to be 4881 km.

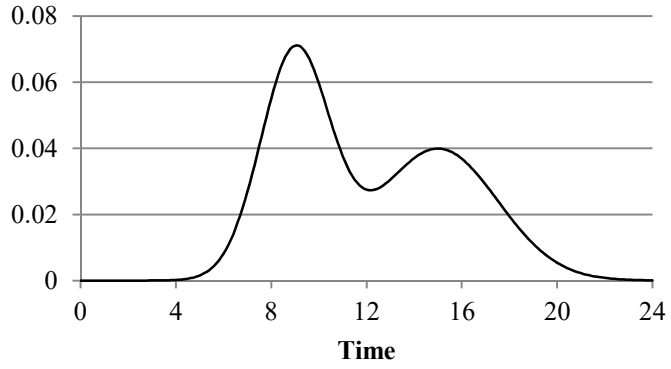

Figure 2. Distribution of non-commuter electric vehicle (EV) departure time.

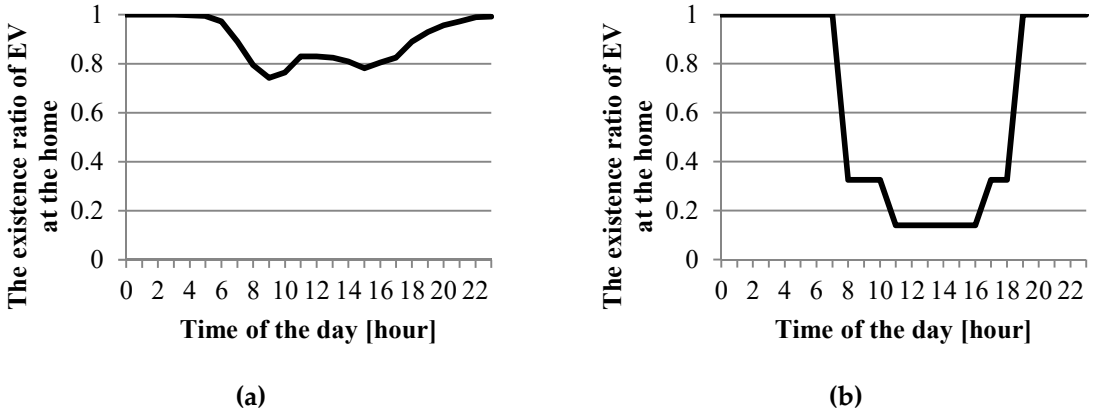

Figure 3. Existence ratio of EVs at home (**a**) non-commuter EV, and (**b**) commuter EV.

The driving pattern of a commuter car is assumed empirically, i.e., the EV is absent from 9:00 a.m to 7:00 p.m. on weekdays and from 12:00 a.m. to 5:00 p.m. on Saturdays and holidays and travels 30 km/day. Figure 3b shows the existence ratio of the commuter EV at home. The annual mileage of the commuter EV is estimated to be 9390 km. According to the analysis based on a nationwide survey in Japan [13], the average mileage of private cars is approximately 9300 km/year, and the mileage of only short-range cars including most non-commuter cars is below approximately 5475 km/year. Therefore, the EV mileage estimated in this case study is considered to be adequate.

The assumed characteristics of EV are shown in Table 2. The power demand of the non-commuter and commuter EVs, $D_{EV}(t)$, can be calculated by their driving pattern and the vehicle efficiency shown in Table 2, and are shown in Figure 4a and b, respectively. The upper limit and lower limit of SoC are empirically set to avoid battery deterioration.

Table 2. Characteristics of EV.

Vehicle efficiency		7	(km/kWh)
Capacity of EV battery	($Cap._{EV}$)	40	(kWh)
Ratio of initial SoC	($r_{EV\_ini.}$)	0.5	
Lower limit of SoC	(lb_{EV_SOC})	8	(kWh)
Upper limit of SoC	(ub_{EV_SOC})	32	(kWh)

The yearly total of the residential power demand is approximately 5311 kWh based on the average of the detached houses [14]. Figure 5 shows the time variation of the residential demand, $D_{home}(t)$, estimated using previously presented information [15]. Figure 6 shows the PV power generation curve per unit capacity, $P_{PV\_unit}(t)$, estimated from solar radiation data [16] for Nagoya city, where the capacity factor of the PV is 13.98%.

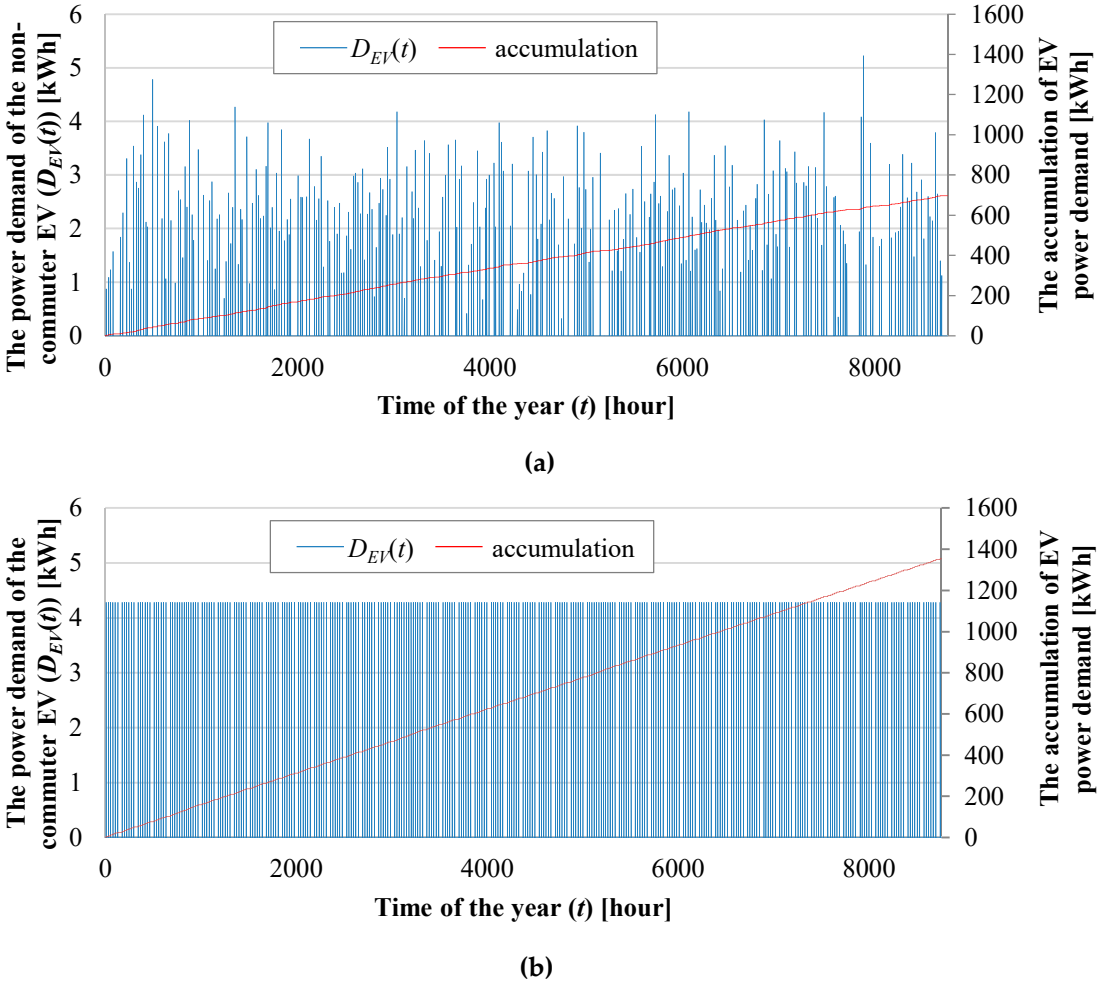

Figure 4. Power demand of EV (**a**) non-commuter EV, and (**b**) commuter EV.

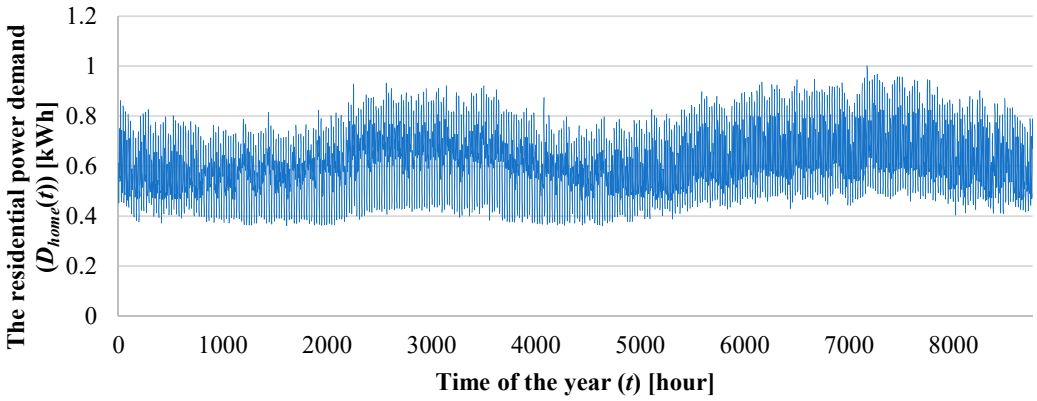

Figure 5. Residential power demand.

The system parameters of PV, SB, and the bidirectional charger for V2H, in 2030, are shown in Table 3. The costs of PV refer to the 2030 forecast provided by the Power Generation Cost Verification Working Group [17]. The costs of the SB are assumed based on previously presented information [18], where the investment cost is approximately a quarter of the current market price in Japan [19]. The charging or discharging power ratio ($r_{SB\_Ch.}$, $r_{SB\_DisCh.}$) is set to 0.333, which is the average value of residential batteries in the current Japanese market [20] (i.e., 3 h to fully charge or discharge battery). A lithium ion battery is considered for these characteristics of SB. The costs of the bidirectional charger for V2H are assumed to differ as per different scenarios, ranging from the current typical price [21] to

one third of the current price. The charging and discharging maximum power of the EV ($P_{EV\_Ch.}$ and $P_{EV\_DisCh.}$) are assumed to be identical to that of a normal charger in Japan.

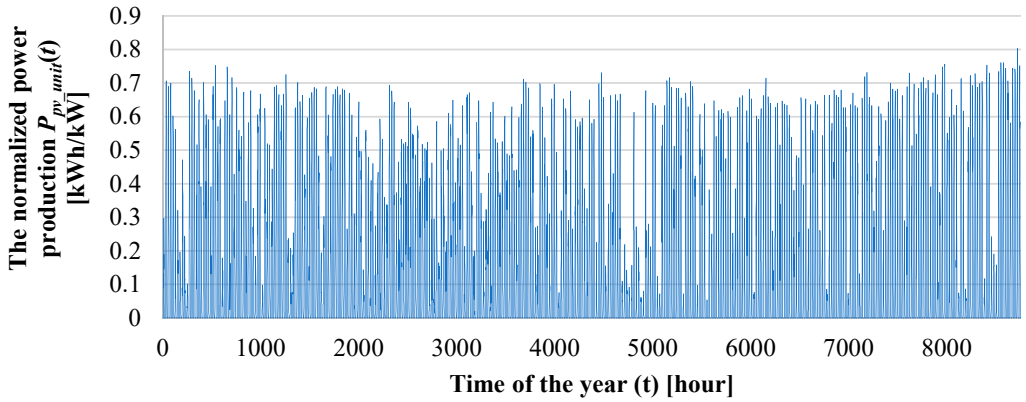

Figure 6. Normalized power production of photovoltaic (PV).

Table 3. System parameters of equipment.

Equipment	Parameter			
PV	*Investment cost*	(I_{PV})	2064	(€/kW)
	Maintenance cost	(M_{PV})	1% of I_{PV}	(€/kW/year)
	Product life	(L_{PV})	30	(year)
	Maximum size	(PV_{max})	10	(kW)
SB	*Investment cost*	(I_{SB})	240	(€/kWh)
	Maintenance cost	(M_{SB})	2% of I_{SB}	(€/kWh/year)
	Product life	(L_{SB})	10	(year)
	Maximum size	(SB_{max})	15	(kWh)
	Efficiency of charging	($\eta_{SB\_Ch.}$)	1.0	
	Efficiency of discharging	($\eta_{SB\_DisCh.}$)	0.86	
	Ratio of initial SoC	($r_{SB\_ini.}$)	0.5	
	Ratio of charging power	($r_{SB\_Ch.}$)	0.333	
	Ratio of discharging power	($r_{SB\_DisCh.}$)	0.333	
Charger or Discharger for EV	*Investment cost*	(I_{V2H})	3600, 2400, 1200	(€/unit)
	Maintenance cost	(M_{V2H})	2% of I_{V2H}	(€/unit/year)
	Product life	(L_{V2H})	10	(year)
	Efficiency of charging	($\eta_{EV\_Ch.}$)	0.9	
	Efficiency of discharging	($\eta_{EV\_DisCh.}$)	0.9	
	Maximum charging power	($P_{EV\_Ch.}$)	3.3	(kW)
	Maximum discharging power	($P_{EV\_DisCh.}$)	3.3	(kW)

The electricity price of grid $p_{buy}(t)$ is assumed to be the minimum unit price for domestic customers offered by the Chubu Electric Power company (0.185 €/kWh) [22]. The selling unit price, $p_{sell}(t)$, is assumed to be 0.04 €/kWh. The adopted CO_2 emission rate for grid power was assumed to be the Japanese target value for the year 2030 [23], i.e., 0.37 kg-CO_2/kWh. The price and CO_2 efficiency of the grid are assumed to be constant values. Therefore, we ignored the economic impact of SB and V2H due to fluctuations in electricity prices. In other words, we focus on the efficiency of SB and V2H for self-consumption of PV power.

3. Results

Figure 7 shows the Pareto solution of the cost and amount of CO_2 emissions for the cases of non-commuter EV. Due to the limited number of calculations, these curves are approximation to the exact Pareto curves [24]. For each curve in Figure 7, the left ends were the results of cost minimization (w = 1) and the right ends show the results of CO_2 emission minimization (w = 0). We ensured that the

Pareto curves of cases 3 and 4 did not intersect when the investment cost of the bidirectional charger was one third the current cost (i.e., I_{V2H} is 1200 €/unit). V2H could reduce CO_2 emissions and energy costs as compared with SB, if the cost of the bidirectional charger was one third of the current cost. However, when the bidirectional charger cost more than two-thirds of the current cost, the economic and environmental performance of V2H is lower than that of SB. Figure 8 shows the cost structure and the optimum sizes of PV and SB, with respect to the results of cost minimization. Case 4 has 6.5 kW of PV, which is the largest as compared to other cases. According to Equation (33), if there is no excess PV generation, the levelized cost of electricity [25] of PV ($LCOE_{PV}$) is calculated as 0.073 €/kWh, which is lower than the purchase unit price from the grid. In Equation (36), C_{PV} is calculated by Equation (3), and the discount rate is not considered in this study (see Appendix A for details).

$$LCOE_{PV} = \frac{C_{PV} * 8760}{\sum_{t=1}^{8760} P_{PV\_unit}(t)} \quad (36)$$

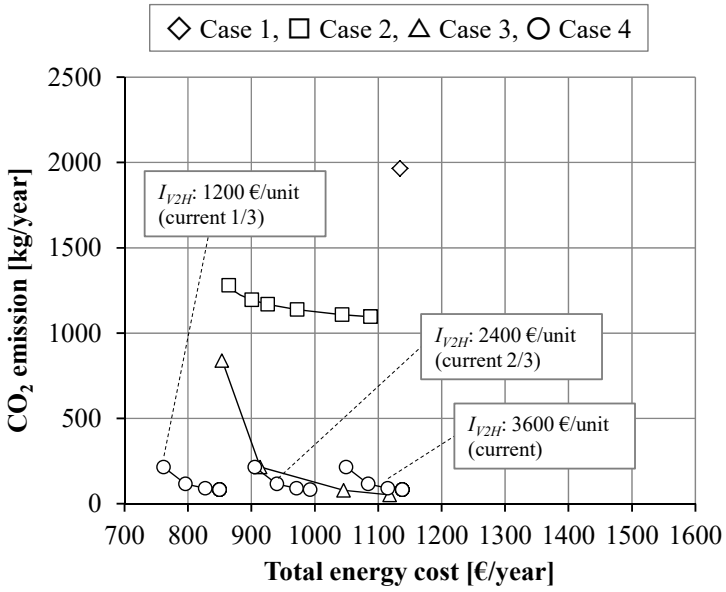

Figure 7. Pareto solution of the cost and amount of CO_2 emission for the cases of non-commuter EV.

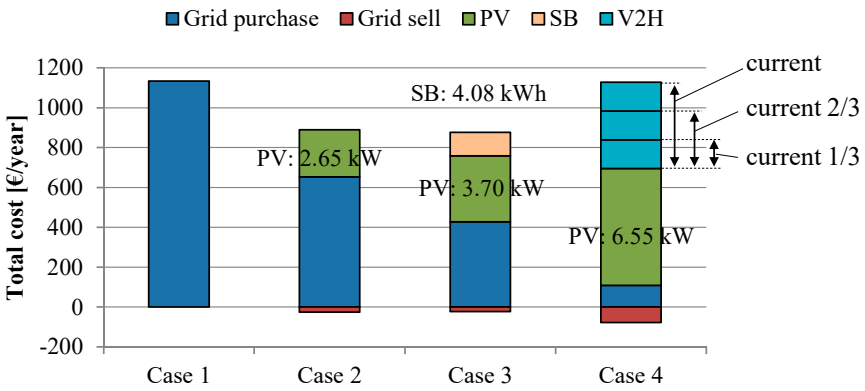

Figure 8. Cost structure and the optimum sizes of PV and stationary battery (SB) of the minimum cost solution for the cases of non-commuter EV.

If excess electricity is generated by increasing the size of PV, cost reduction will be possible by preventing a decrease in the utilization rate of PV power generation with an inexpensive storage. There are many opportunities for non-commuter EVs to charge PV.

Figures 9–12 show the relationship between the residential supply-demand balance and the operation schedule of the batteries (EV and SB) on some specific days as examples of the optimized schedule in the minimum cost solution. The results of cases 3 and 4 on the day with a large amount of PV power generation (October 1) are shown in Figures 9 and 10, respectively. From Figure 9a, in case 3, daytime residential power demand was met using PV, and excess power was used to charge the SB and EV. The SB discharged in the evening and grid power was purchased at night. From Figure 9b, the SoC of EV battery was sufficient for driving, and the EV was charged while at home. From Figure 9c, the SoC of SB circulated from empty to full charge in one day. As shown in Figure 10a, in case 4, the excess power generation was used to charge the EV and the residential power demand was met by V2H at night. From Figure 10b, with the use of V2H, the SoC of EV battery increased or decreased significantly in one day. In contrast, Figures 11 and 12 show the energy flows in cases 3 and 4 on October 2, when PV power generation is low. As shown in Figure 11a,c, because excess PV power was low, charging and discharging of the SB was slight and the EV was not charged in case 3. From Figure 11b, the SoC of the EV battery was found to be sufficient for the driving demand, hence, the SB was preferentially charged on this day. From Figure 12a,b, in case 4, there was limited excess power generation, however, V2H could satisfy the residential power demand without purchasing grid power. Therefore, in case 4, we found that the EV batteries with a larger storage capacity than the SB encouraged the use of excess PV power at night when bidirectional chargers were of low cost.

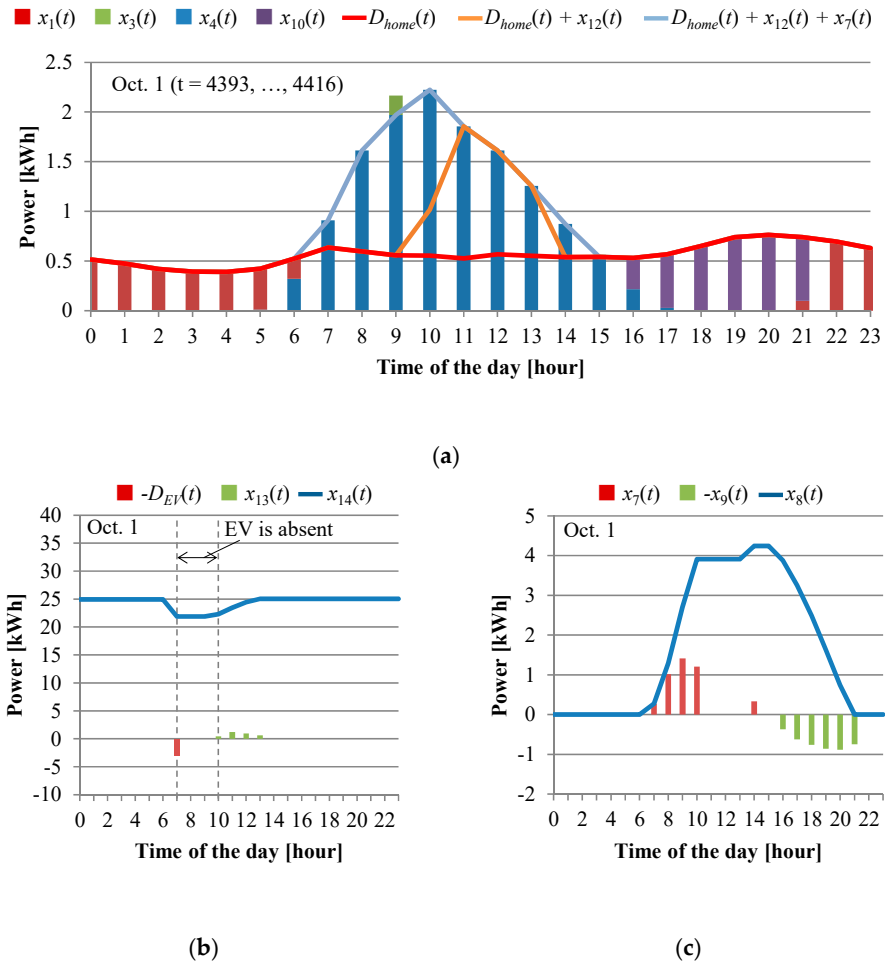

Figure 9. Optimized energy flow in case 3 on the day with large amount of PV power generation (**a**) residential supply-demand balance, (**b**) operation schedule of EV battery, and (**c**) operation schedule of SB.

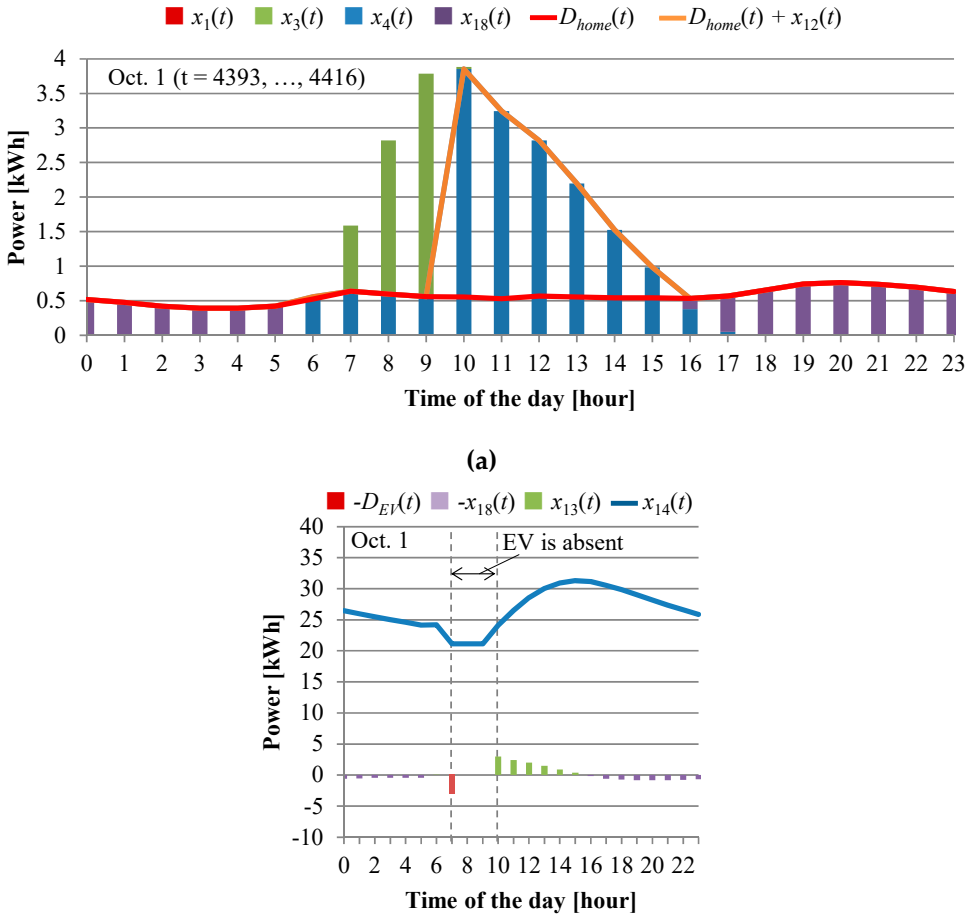

Figure 10. Optimized energy flow in case 4 on the day with large amount of PV power generation (**a**) residential supply-demand balance and (**b**) operation schedule of EV battery with vehicle-to-home (V2H).

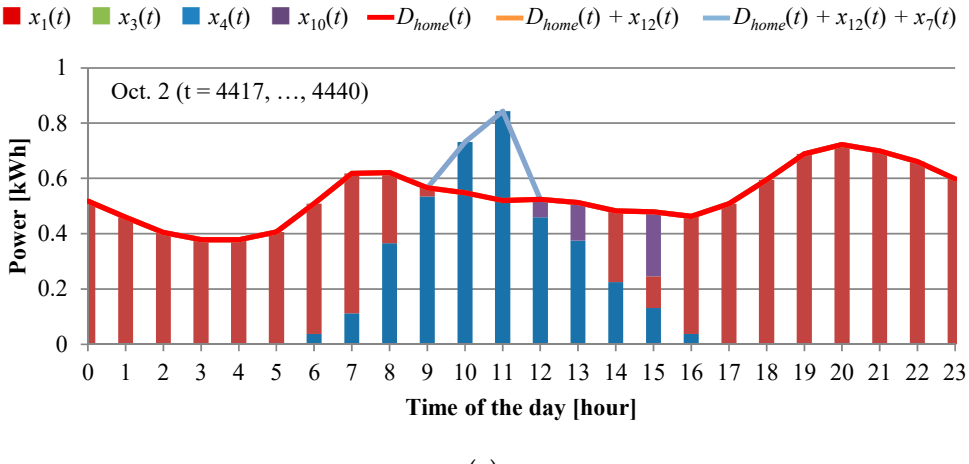

Figure 11. *Cont.*

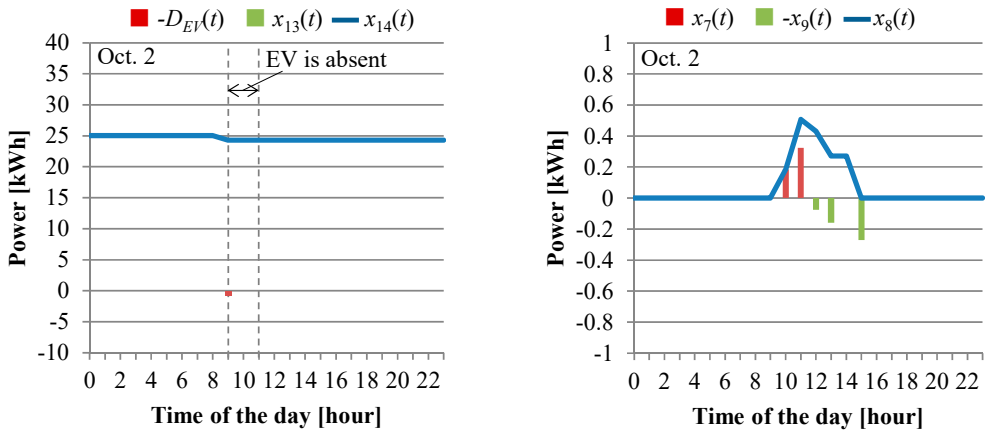

(**b**) (**c**)

Figure 11. Optimized energy flow in case 3 on the day with small amount of PV power generation (**a**) residential supply-demand balance, (**b**) operation schedule of EV battery, and (**c**) operation schedule of SB.

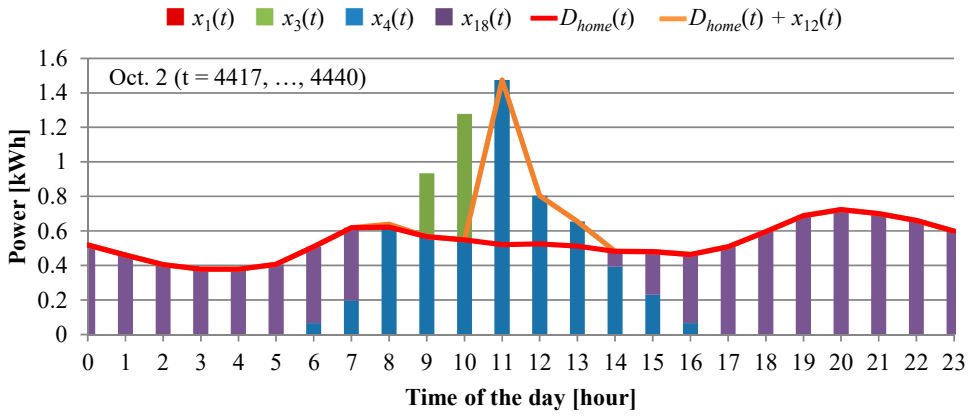

(a)

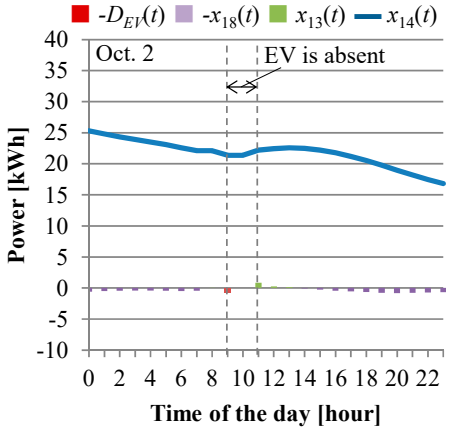

(b)

Figure 12. Optimized energy flow in case 4 on the day with small amount of PV power generation (**a**) residential supply-demand balance and (**b**) operation schedule of EV battery with V2H.

Focusing on CO_2 minimization, Figure 13 shows that the PV and SB sizes reached the installation upper limits to reduce the use of grid power as far as possible. The self-consumption rate, r_{sc}, shown in Figure 9 is calculated by Equation (37).

$$r_{sc} = 1 - \sum_{t=1}^{T} \frac{x_1(t)}{D_{home}(t) + D_{EV}(t)/\eta_{EV\_Ch.}} \quad (37)$$

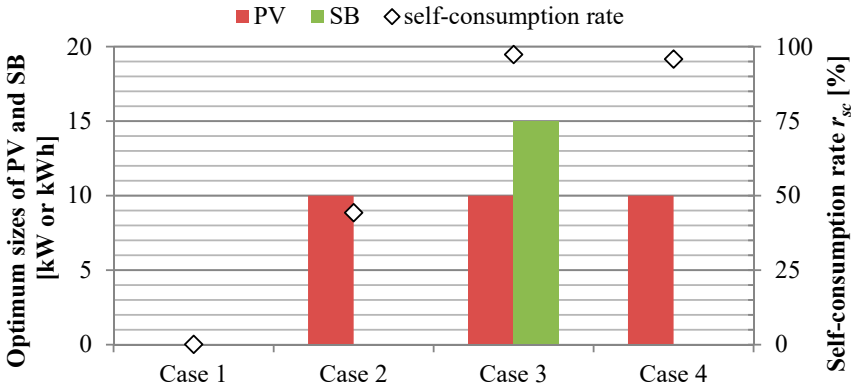

Figure 13. Self-consumption rate and optimum sizes of PV and SB.

The self-consumption rate in case 2 is approximately 50% because the PV is used at daytime. In case 3 and case 4, the self-consumption rate is over 90% because battery discharge is added at night. Although the battery capacity of the EV is larger than that of SB, the minimum CO_2 emission in case 4 is larger than that in case 3. Under the conditions applied in this study, it is found that the SB with a capacity of 15 kWh can charge excess PV more than the EV because of the probability of the absence of EV.

Figure 14 shows the Pareto solution of the cost and amount of CO_2 emission for the cases of commuter EV. In the case of a commuter car, the tendency of cases 5, 6, and 7 is similar to the case of a non-commuter car. However, in case 8, it is clear that even if the cost of V2H is one third the current cost, it is inferior in environmental and economic performance as compared to case 7. This is because the probability of absence during the day time is high and power generation from PV cannot be charged.

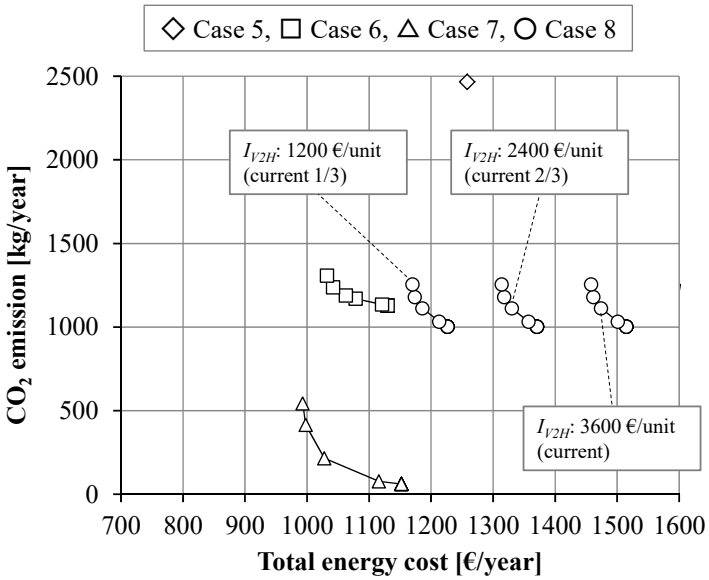

Figure 14. Pareto solution of the cost and amount of CO_2 emission for the cases of commuter EV.

4. Discussion

In the case of non-commuter cars, we found that if the cost of a bidirectional charger for V2H is one-third the current cost or less, it is economically and environmentally superior to SB. Recently, it was reported that bidirectional chargers will be sold at approximately half their prices because of cost reduction [26], but if the SB cost is assumed to be low, as in this study, it is necessary to further reduce the cost of V2H to motivate EV owners to use V2H. In contrast, in the case of a commuter car, there is no merit in introducing V2H even if the cost is one third the current cost because the EV is absent in the daytime and cannot be charged by solar power. Furthermore, as shown in Figure 4, even if the cost of the bidirectional charger is zero, it can be estimated that there is no significance in introducing V2H. In other words, the probability of the EV staying at home greatly affects the effectiveness of V2H, and therefore a dissemination strategy that considers the target user's driving pattern is necessary. In future work, the analysis of V2H superiority based on the driving data of diverse EV using the method used in this study could help motivate EV owners to install V2H. In addition, to get an overview of the trends, a parameter study that considers aspects such as the following is required: fluctuations in the grid power price, the cost of PV and SB, the size of the EV battery, and the charge/discharge power of EV.

5. Conclusions

In this study, we developed a multi-objective optimization method to evaluate the economic and environmental performance of V2H using the energy costs including investment in equipment and CO_2 emissions as indices. We evaluated the economic and environmental efficiency of a typical EV owner's detached house in Japan as a case study and compared the performance of V2H and SB. As a result, we found that V2H could be better than the low-price SB, in 2030, for non-commuting EV owners if the investment cost of a bidirectional charger is one third the current cost. In contrast, in the case of a commuting EV, V2H would not be economically and environmentally rational because the EV is absent during the daytime. The results of this study will contribute to the rational setting of investment costs for spread and the selection of EV owners to invest in V2H. In future work, we could evaluate additional future scenarios regarding diverse driving patterns using our optimization framework for fluctuations in the grid power price, the cost of PV and SB, the size of the EV battery, and the charge/discharge power of EV.

Author Contributions: Conceptualization, R.K.; Data curation, R.K.; Formal analysis, R.K. and H.Y.; Investigation, R.K.; Methodology, R.K.; Project administration, A.S.; Supervision, A.S.; Validation, R.K.; Writing—original draft, R.K.; Writing—review & editing, A.S., Y.I. and K.O.

Funding: This research received no external funding.

Conflicts of Interest: The authors declare no conflict of interest.

Nomenclature

Set	
t	index of optimization periods, t = 1, 2, ..., T (hour)
Variables	
$x_i(t)$ (i = 1, ..., 19)	energy flow or state of charge in period t (kWh)
y_2	size of PV (kW)
y_8	size of SB (kWh)
z_{18}	necessity of V2H system (binary variable) (unit)
f_{cost}	total energy cost (€)
f_{CO2}	total CO_2 emission (kg-CO_2)

Parameters

T	time horizon of the optimization problem (hour)
$p_{buy}(t)$	purchase unit price in period t (€/kWh)
$p_{sell}(t)$	selling unit price in period t (€/kWh)
C_{PV}	cost coefficients of PV (€/kW/hour)
C_{SB}	cost coefficients of SB (€/kWh/hour)
C_{V2H}	cost coefficients of V2H (€/unit/hour)
I_{PV}	investment cost of PV (€/kW)
I_{SB}	investment cost of SB (€/kWh)
I_{V2H}	investment cost of V2H (€/unit)
M_{PV}	annual maintenance cost of PV (€/kW/year)
M_{SB}	annual maintenance cost of SB (€/kWh/year)
M_{V2H}	annual maintenance cost of V2H (€/unit/year)
L_{PV}	product life of PV (year)
L_{SB}	product life of SB (year)
L_{V2H}	product life of V2H (year)
e_{grid}	CO_2 emission rate for grid power (kg-CO_2/kWh)
$P_{PV\_unit}(t)$	normalized power production of PV in period t (kWh/kW)
$D_{EV}(t)$	power demand to drive EV in period t (kWh)
$D_{home}(t)$	residential power demand in period t (kWh)
$Cap._{EV}$	capacity of EV battery (kWh)
$r_{EV\_ini.}$	ratio of initial SoC
lb_{EV_SOC}	lower limit of SoC (kWh)
ub_{EV_SOC}	upper limit of SoC (kWh)
PV_{max}	maximum size of PV (kW)
SB_{max}	maximum size of SB (kW)
$\eta_{SB\_Ch.}$	efficiency of charging for SB
$\eta_{SB\_DisCh.}$	efficiency of discharging for SB
$r_{SB\_ini.}$	ratio of initial SoC for SB
$r_{SB\_Ch.}$	ratio of charging power for SB
$r_{SB\_DisCh.}$	ratio of discharging power for SB
$\eta_{EV\_Ch.}$	efficiency of charging for EV
$\eta_{EV\_DisCh.}$	efficiency of discharging for EV
$P_{EV\_Ch.}$	charging power for EV (kW)
$P_{EV\_DisCh.}$	discharging power for EV (kW)
$\delta_{EV}(t)$	the absence of the EV in period t
DT	departure time (hour)
CT	comeback time (hour)
ST	stay time (min)
DP	driving period (min)
TL	trip length (km)
V	average driving speed of EV (km/h)
w	weight of objectives

Appendix A

The formula of the levelized cost of electricity is defined by International Renewable Energy Agency as follow [25]:

$$LCOE = \frac{\sum_{i=1}^{n} \frac{I_i + M_i + F_i}{(1+r)^i}}{\sum_{i=1}^{n} \frac{E_i}{(1+r)^i}} \quad \text{(A1)}$$

where:

$LCOE$ = the levelized cost of electricity;
I_i = investment expenditures in the year i;

M_i = operations and maintenance expenditures in the year i;
F_i = fuel expenditures in the year i;
E_i = electricity generation in the year i; r = discount rate; and
n = life of the system.

Based on Equation (A1), $LCOE_{PV}$ was formulated into Equation (36) in the main text with the following process. The variables in Equation (A1) can be rewritten using the following nomenclature in Section 2: $I_i = I_{PV}/L_{PV}$, $M_i = M_{PV}$, $E_i = \sum_{t=1}^{8760} P_{PV\_unit}(t)$, and $n = L_{PV}$. The PV needs no fuel, $F_i = 0$ and the discount rate is assumed to be zero in this study, $r = 0$. Therefore,

$$LCOE_{PV} = \frac{\sum_{i=1}^{L_{PV}} \left(\frac{I_{PV}}{L_{PV}} + M_{PV}\right)}{\sum_{i=1}^{L_{PV}} \sum_{t=1}^{8760} P_{PV\_unit}(t)} \quad \text{(A2)}$$

I_{PV}, L_{PV}, M_{PV} and $P_{PV\_unit}(t)$ are independent of the year i:

$$LCOE_{PV} = \frac{L_{PV}\left(\frac{I_{PV}}{L_{PV}} + M_{PV}\right)}{L_{PV} \sum_{t=1}^{8760} P_{PV\_unit}(t)} = \frac{\left(\frac{I_{PV}}{L_{PV}} + M_{PV}\right)}{\sum_{t=1}^{8760} P_{PV\_unit}(t)} \quad \text{(A3)}$$

As a result of substituting C_{PV} in Equation (3) into Equation (A3), Equation (A4) matches Equation (36).

$$LCOE_{PV} = \frac{C_{PV} * 8760}{\sum_{t=1}^{8760} P_{PV\_unit}(t)} \quad \text{(A4)}$$

References

1. Ministry of Economy, Trade and Industry. *The 5th Strategic Energy Plan*; METI: Tokyo, Japan, 2018. Available online: https://www.enecho.meti.go.jp/en/category/others/basic_plan/5th/pdf/strategic_energy_plan.pdf (accessed on 1 October 2019).
2. Kaschub, T.; Jochem, P.; Fichtner, W. Interdependencies of Home Energy Storage between Electric and Stationary Battery. *World Electr. Veh. J.* **2013**, *6*, 1144–1150. [CrossRef]
3. Erdinc, O.; Paterakis, N.G.; Mendes, T.D.P.; Bakirtzis, A.G.; Catalao, J.P.S. Smart Household Operation Considering Bi-directional EV and ESS Utilization by Real-Time Pricing-Based DR. *IEEE Trans. Smart Grid* **2015**, *6*, 1281–1291. [CrossRef]
4. Wu, X.; Hu, X.; Moura, S.; Yin, X.; Pickert, V. Stochastic control of smart home energy management with plug-in electric vehicle battery energy storage and photovoltaic array. *J. Power Sources* **2016**, *333*, 203–212. [CrossRef]
5. Erdinc, O.; Paterakis, N.G.; Pappi, I.N.; Bakirtzis, A.G.; Catalao, J.P.S. A new perspective for sizing of distributed generation and energy storage for smart households under demand response. *Appl. Energy* **2015**, *143*, 26–37. [CrossRef]
6. Wu, X.; Hu, X.; Teng, Y.; Qian, S.; Cheng, R. Optimal integration of a hybrid solar-battery power source into smart home nanogrid with plug-in electric vehicle. *J. Power Sources* **2017**, *363*, 277–283. [CrossRef]
7. Naghibi, B.; Masoum, M.A.S.; Deilami, S. Effects of V2H Integration on Optimal Sizing of Renewable Resources in Smart Home Based on Monte Carlo Simulations. *IEEE Power Energy Technol. Syst. J.* **2018**, *5*, 73–84. [CrossRef]
8. Technology Collaboration Programme on Hybrid and Electric Vehicles (HEV TCP). *Hybrid and Electric Vehicles -The Electric Drive Hauls-*; International Energy Agency: Paris, France, 2019; pp. 67–73. Available online: http://www.ieahev.org/assets/1/7/Report2019_WEB_New_(1).pdf (accessed on 1 October 2019).
9. Zakariazadeh, A.; Jadid, S.; Siano, P. Multi-objective scheduling of electric vehicles in smart distribution system. *Energy Convers. Manag.* **2014**, *79*, 43–53. [CrossRef]
10. Kataoka, R.; Shichi, A.; Yamada, H.; Iwafune, Y.; Ogimoto, K. Evaluation of Economic and Environmental Superiority of EV Battery in Power Systems: Development of Multi-objective Optimized Model for V2H. In Proceedings of the 32nd Electric Vehicle Symposium (EVS32), Lyon, France, 19–22 May 2019.

11. MathWorks, Optimization Toolbox. Available online: https://jp.mathworks.com/help/optim/index.html?lang=en (accessed on 1 October 2019).
12. Mustapha, A.; Fonseca, J.G.D.S., Jr.; Oozeki, T.; Iwafune, Y. Evaluation of Residential PV-EV System for Supply and Demand Balance of Power System. *IEEJ Trans. Power Energy* **2015**, *135*, 27–34. (In Japanese) [CrossRef]
13. Iwafune, Y.; Ogimoto, K.; Azuma, H. Integration of Electric Vehicles into the Electric Power System Based on Results of Road Traffic Census. *Energies* **2019**, *12*, 1849. [CrossRef]
14. The Energy Conservation Center, Japan. Results of the Survey of Standby Power Consumption. 2013. (In Japanese)
15. Morita, K.; Manabe, Y.; Kato, T.; Funabashi, T.; Suzuoki, Y. An Evaluation of Average Electricity Demand Characteristics with Hundreds of Households. *J. Jpn. Soc. Energy Resour.* **2016**, *38*, 20–29. (In Japanese) [CrossRef]
16. New Energy and Industrial Technology Development Organization, MEteorological Test data for PhotoVoltaic System. Available online: http://www.nedo.go.jp/library/nissharyou.html (accessed on 1 October 2019).
17. Power Generation Cost Analysis Working Group, Report on Analysis of Generation Costs, Etc. for Subcommittee on Long-term Energy Supply- demand Outlook. 2015. Available online: https://www.meti.go.jp/english/press/2015/pdf/0716_01b.pdf (accessed on 1 October 2019).
18. Kobashi, T.; Say, K.; Wang, J.; Yarime, M. Techno-economic analyses of PV, PV + battery, PV + EV for household in Kyoto and Shenzhen towards 2030. In Proceedings of the 35th Energy Systems Economic Environment Conference, Tokyo, Japan, 30 January 2019; pp. 383–386. (In Japanese).
19. Ministry of Economy, Trade and Industry. Available online: http://www.meti.go.jp/committee/kenkyukai/energy_environment/energy_resource/pdf/005_08_00.pdf (accessed on 1 October 2019).
20. Mitsubishi Research Institute, Inc. 2017. Available online: https://www.meti.go.jp/meti_lib/report/H28FY/000479.pdf (accessed on 1 October 2019).
21. Nichicon Corp., EV Power Station. Available online: https://www.nichicon.co.jp/products/v2h/about/ (accessed on 1 October 2019).
22. Chubu Electric Power Co. Inc. Available online: http://www.chuden.co.jp/home/home_menu/home_basic/otoku/index.html (accessed on 1 October 2019).
23. The Federation of Electric Power Companies of Japan, Expanding Use of Non-Fossil Energy Sources. Available online: https://www.fepc.or.jp/english/environment/global_warming/nuclear_lng/ (accessed on 1 October 2019).
24. Hara, T. Technology Assessment based on Range Analysis of the Linear-Programming Bottom-up Energy Systems Model. *J. Jpn. Soc. Energy Resour.* **2019**, *40*, 202–219. (In Japanese) [CrossRef]
25. International Renewable Energy Agency; Data Methodology. 2015. Available online: http://dashboard.irena.org/download/Methodology.pdf (accessed on 1 October 2019).
26. Landi, M. Vehicle-to-Grid developments in the UK. In Proceedings of the 32nd Electric Vehicle Symposium (EVS32), Lyon, France, 19–22 May 2019.